

Effects of Damper Layer Parameters on Applied Strain Uniformity in Static Elastography

静的エラストグラフィにおける緩衝層挿入による歪み均一化の実験的検証

Yuichi Tashiro^{1†}, Takayuki Sato¹ (¹ Grad. School of Sci. and Eng., Tokyo Metropolitan Univ.)

田代 祐一[†], 佐藤 隆幸¹ (¹ 首都大院 理工)

1. Introduction

Static elastography¹⁻²⁾ is expected to be mainly used to diagnose breast cancer. Recently, target of the elastography is extended to diagnoses liver, muscle and so on. However, the elasticity estimated by the static elastography strongly depends on the applied stress distribution. An effective method of improving the nonuniformity of applied stress that occurs with different shapes of the transducer head is to insert a damper between the tissue being analyzed and the transducer head³⁻⁴⁾.

In this study, the effects of the damper parameters on the applied strain uniformity was studied.

2. Experimental Method

As Fig.1 shows, The convex-shaped phantom consisted of a truncated sphere with a 9 cm radius and a 6 cm diameter of a cylinder. The phantom was produced from a 1.4 wt% agar solution with the dispersion of 0.5 wt% graphite powder with the diameter of 50 μm.

Two plain-shaped dampers inserted between the phantom and the transducer head were produced, namely, a 1.0 wt%-agar damper with the thickness of 5 mm and a 0.8 wt%-agar damper with the thickness of 10 mm. The Young' moduli of the three agar samples produced with the agar concentrations of the 0.8, 1.0 and 1.4 wt% without the graphite powder were estimated as 25, 37 and 72 kPa, respectively.

An experimental setup, which was able to compress the phantom and acquire the echo signal, was illustrated in Fig.2. A 128 ch linear array transducer with the center frequency of 10MHz was attached flat to the compression board. The initial compression⁴⁾ stroke along this center axis was defined as 2.3mm, which is long enough for the observation width of transducer to be in contact with the convex tissue surface as drawn in Fig.3. Additionally, the secondary compression, that is,

1% of the thickness of the compressed tissue.

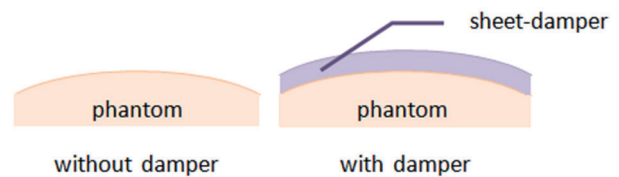


Fig. 1 Cross section of phantom and sheet-damper

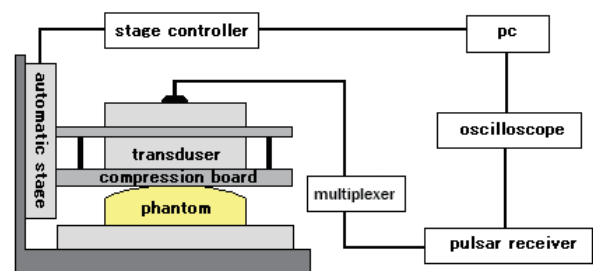


Fig. 2 Block diagram of experiment setup

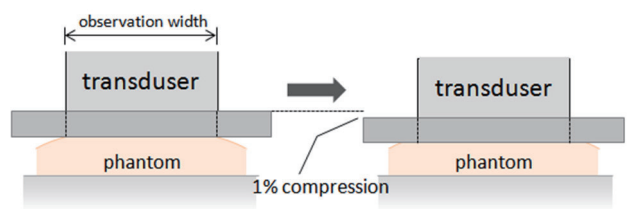


Fig. 3 Boundary conditions of phantom compression

The estimation of the strain distribution inside the phantom was based on the cross-correlational process executed between the echo signals obtained the pre- and post- compressions.

The correlation coefficients given by

$$\rho = \frac{\sum_{i=i_0-M/2}^{i_0+M/2} (a_i - \bar{a})(b_{i+l} - \bar{b})}{\sqrt{\sum_{i=i_0-M/2}^{i_0+M/2} |a_i - \bar{a}|^2 \sum_{i=i_0-M/2}^{i_0+M/2} |b_{i+l} - \bar{b}|^2}} \quad (1),$$

were sequentially calculated to detect the maximally-correlated points between the two echo signals. The displacement was defined as the difference between the maximally-correlated points. The strain distribution was obtained by differentiating the displacements.

3. Results

Figure 4 show the estimated strain distributions inside the phantom in the cases of without the damper, with the thin and hard damper, and the soft and thick damper, respectively. Obvious differences between the axial strain directly under the center of the transducer and the strain directly under the edge of the transducer at the same depth were observed in Fig. 4 (a), thus, the strain uniformity in the lateral direction was low. In the cases of with the dampers, i.e., in Figs. 4 (b) and (c), the strain uniformity was observed to be improved. In particular, as shown in Fig. 4 (c), a more desirable result of the strain uniformity was obtained with the soft and thick damper.

4. Conclusion

The effectiveness of equalizing the applied strain on convex phantom by inserting a damper layer was confirmed by the experiments with damper thickness and Young's modulus as parameters. In our preparatory investigation, a high strain uniformity was expected to be achieved by using the plano-concave damper, so the shape of the damper was also considered to be suitable. The use of this shape of damper would lead to high uniformity of the applied strain distribution in convex parts of the human body.

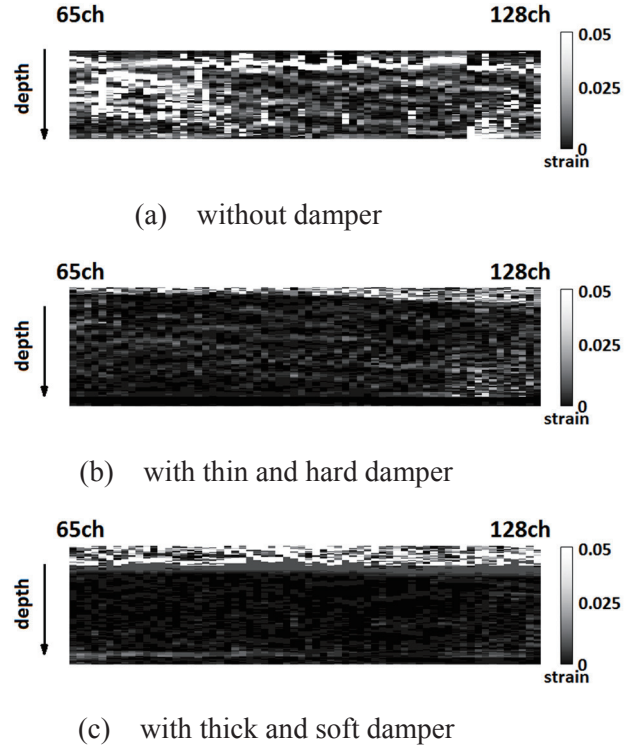


Fig. 4 Distribution of strain inside the phantom

References

1. J. Ophir, El. Ce'spedes, H. Ponnekanti, Y. Yazdi, and X. Li: *Ultrason. Imaging* 13 (1991) 111.
2. N. A. Cohn, S. Y. Emelianov, M. A. Lubinski, and M. O'Donnell: *IEEE Trans. Ultrason. Ferroelectr. Freq. Control* 44 (1997) 1304.
3. T. Sato, S. Sato, Y. Watanabe, S. Goka, and H. Sekimoto: *Jpn. J. Appl. Phys.* 49 (2010) 07HF30.
4. T. Sato, Y. Watanabe, and H. Sekimoto: *Jpn. J. Appl. Phys.* 51 (2012) 07GF16.